

Two Dimensional Diluted Magnetic Semiconductor Systems

D. J. Priour, Jr, E. H. Hwang, and S. Das Sarma

Condensed Matter Theory Center, Department of Physics, University of Maryland, College Park, MD 20742-4111

We develop a theory for two-dimensional diluted magnetic semiconductor systems (e.g. $\text{Ga}_{1-x}\text{Mn}_x\text{As}$ layers) where the itinerant carriers mediating the ferromagnetic interaction between the impurity local moments, as well as the local moments themselves, are confined in a two-dimensional layer. The theory includes exact spatial disorder effects associated with the random local moment positions within a disordered RKKY lattice field theory description. We predict the ferromagnetic transition temperature (T_c) as well as the nature of the spontaneous magnetization. The theory includes disorder and finite carrier mean free path effects as well as the important correction arising from the *finite temperature* RKKY interaction, finding a strong density dependence of T_c in contrast to the simple virtual crystal approximation.

PACS numbers: 75.50.Pp, 75.10.-b, 75.10.Nr, 75.30.Hx

Many projected applications of diluted magnetic semiconductors (DMS), i.e. systems which combine the advantages of a ferromagnetic material with those of a semiconductor with the additional flexibility of carrier-mediated ferromagnetism enabling the tuning of the magnetic properties by applying external gate voltages or optical pulses to control the carrier density, would involve the use of two-dimensional (2D) DMS structures such as quantum wells, multilayers, superlattices, or heterostructures. Such 2D DMS structures are also of intrinsic fundamental interest since magnetic properties in two dimensions are expected to be substantially different from the three dimensional (3D) systems [1] that have mostly been theoretically studied in the DMS literature. The 2D DMS systems introduce the possibility of gating, and thereby controlling both electrical and magnetic properties by tuning the carrier density. In fact, such a carrier density modulation of DMS properties has already been demonstrated [2,3] in gated DMS field effect heterostructures. For various future spintronic applications the development of such 2D DMS structures is obviously of great importance.

In this Letter, we provide the basic theoretical picture underlying 2D DMS ferromagnetism focusing on the well-studied $\text{Ga}_{1-x}\text{Mn}_x\text{As}$, with $x \approx 0.03-0.08$, a system where the ferromagnetism is well-established to be arising from the alignment (for $T < T_c \sim 100\text{K} - 200\text{K}$) of Mn local moments through the indirect exchange interaction carried by itinerant holes in the GaAs valence (or impurity) band (that also contributed by the Mn atoms which serve the dual purpose of being the impurity local moments as well as the dopants). Our theory is quite general and should apply to other “metallic” DMS materials where the ferromagnetic interaction between the impurity local moments is mediated by itinerant carriers (electrons or holes). Our theory is a suitable 2D generalization of both the continuum lattice version of the highly successful RKKY mean field theory (MFT) that has earlier been applied [1] to 3D metallic $\text{Ga}_{1-x}\text{Mn}_x\text{As}$ systems. One of our important findings is that the ferromagnetic

transition (“Curie”) temperature for the 2D DMS systems typically tends to be substantially less than the corresponding 3D case with equivalent system parameters. In particular, T_c in the 2D case is found to be comparable ($T_c \sim T_F$) to the Fermi temperature ($T_F = E_F/k_B$, where E_F is the 2D Fermi energy) of the 2D hole systems. This necessitates that the full finite temperature form for the 2D RKKY interaction be used in calculating DMS magnetic properties, further suppressing T_c in the system. In fact, this general lowering of the 2D DMS T_c compared with the corresponding 3D case is our central new theoretical result. This implies that spintronic applications involving 2D DMS heterostructures will be problematic since the typical T_c (at least for the currently existing DMS materials) is likely to be far below room temperature ($T_c < 100\text{K}$). A related equally important theoretical finding is that, although the continuum virtual crystal mean field approximation much used for 3D $\text{Ga}_{1-x}\text{Mn}_x\text{As}$ physics [4] would predict that the T_c in 2D DMS systems (being proportional to the 2D density of states) is independent of 2D carrier density, there is an *intrinsic* carrier density dependence of T_c even in the strict 2D system arising from the density and temperature (i.e. T/T_F) dependence of the finite-temperature effective RKKY interaction.

We specifically consider the so-called delta-doping schemes for localizing Mn dopants, the species responsible for DMS ferromagnetism, to very narrow layers [3]. It is this situation which we examine in this letter, spin-5/2 Mn impurities confined to a single plane in GaAs; although the experimental reality may well be one in which a significant number of impurities lie off this plane and/or the Mn occupy a different crystallographic plane, our results are qualitatively correct in these cases as well. We apply the lattice MFT developed previously [5], but we also find intriguing results in the context of simple continuum Weiss MFT which demonstrate that it is essential to incorporate finite temperature effects in the effective carrier-mediated interaction between Mn impurity moments. We assume the 2D hole gas to be confined in the

same plane as the Mn dopants— it is straightforward to consider a spatial separation between the dopants and the holes as well as to consider the quasi-2D confinement for the holes. These additional complications would lower T_c below the strict 2D limit considered in our model.

Our theory is constructed for two dimensional DMS systems in the metallic limit with itinerant carriers (we assume the carrier-mediated effective Mn-Mn indirect exchange interaction to be of the RKKY form). However, including a finite carrier mean free path in our theory allows us to take into account the dependence of the magnetic behavior of our system on the carrier transport properties. In fact, using an exponential cutoff in the range of the RKKY function permits us to treat the long and short-range magnetic interaction regimes simply by varying the cutoff parameter l . In our system, salient parameters include the Mn local moment concentration (x), the free carrier density (n_c), and the exponential cutoff scale l associated with the carrier mean free path. The 2D Fermi temperature $T_F = \frac{\hbar^2 k_F^2}{2m^* k_B}$ depends on n_c since the 2D $k_F \propto n_c^{1/2}$, where k_F is the Fermi wave vector. We take the carrier effective mass to be $m^* = 0.4m_e$ for all our numerical results. All quantities (T_F, k_F, r , etc.) appearing in our theory refer to 2D parameters.

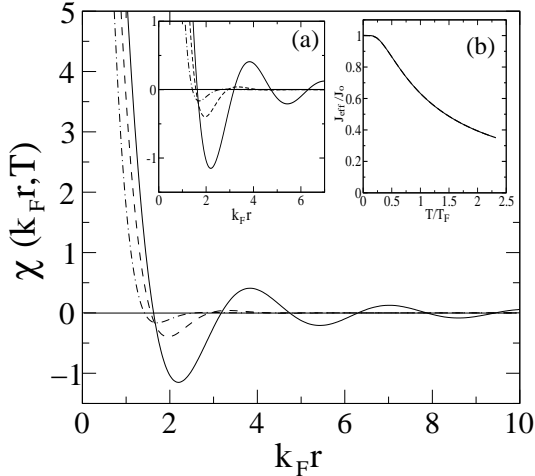


FIG. 1. Temperature dependent 2D RKKY range function $\chi(k_F r, T/T_F)$ as a function of $k_F r$ for several temperatures $T/T_F = 0.0, 0.5$, and 1.0 (corresponding to the solid, dashed, and dot dashed lines respectively). Inset (a) also shows $\chi(k_F r, T/T_F)$, and inset (b) portrays the effective finite temperature coupling J_{eff} .

Our effective Hamiltonian describes the Mn-Mn magnetic interaction between classical Heisenberg spins \mathbf{S}_i on a 2D lattice:

$$\mathcal{H} = \sum_{ij} J_{ij}^{\text{RKKY}} \mathbf{S}_i \cdot \mathbf{S}_j \quad (1)$$

where \mathbf{S}_i is the i th Mn local moment of spin $5/2$. In our lattice MFT we assume the Mn dopants to lie entirely on the $[100]$ plane of the GaAs zinc-blende crystal lattice,

with the impurities occupying the Ga sites, which form a square lattice with lattice constant a .

In our Hamiltonian, the carrier mediated RKKY indirect exchange interaction describes the effective magnetic interaction between Mn local moments induced by the free carrier spin polarization. $J_{ij}^{\text{RKKY}}(T) \equiv \mathcal{J}_0 \chi(k_F r, T/T_F)$, where $\chi(k_F r, T/T_F)$ is the temperature dependent range function which is obtained from the 2D spin susceptibility, and $\mathcal{J}_0 \equiv \left[\frac{J_{pd}}{a} \right]^2 \frac{m^*}{8[\pi\hbar]^2 a^2}$. Taking $J_{pd} = 0.15 \text{ eVnm}^3$ [6] and square lattice constant $a = .4 \text{ nm}$, we find $\mathcal{J}_0 = 0.10 \text{ eV}$; we use this value for \mathcal{J}_0 throughout this work.

For $T = 0$ the 2D RKKY interaction is known exactly [7]:

$$J_{ij}^{\text{RKKY}} \equiv \mathcal{J}_0 (k_F a)^2 [J_0(k_F r) N_0(k_F r) + J_1(k_F r) N_1(k_F r)] \quad (2)$$

where $J_n(x)$ are the Bessel functions of the first kind, and $N_n(x)$ are Bessel functions of the second kind. The asymptotic form of the RKKY interaction for $k_F r \gg 1$ is $J^{\text{RKKY}}(r) \propto \mathcal{J}_0 \sin(2k_F r)/r^2$. At finite temperatures (i.e., for $T/T_F \neq 0$), it is not possible to obtain the RKKY range function analytically. Thus, we calculate the finite temperature RKKY interaction numerically. In Fig. 1, we show the temperature dependent range function $\chi(k_F r, T/T_F)$ as a function of $k_F r$ for various T/T_F values. One sees increasingly severe thermal damping of the RKKY oscillations with increasing T/T_F . Inset (a) of Fig. 1 provides a closer view of the RKKY oscillations depicted in the main graph, while inset (b) displays the effective coupling constant, given by $J_{\text{eff}} = \int J_{ij}^{\text{RKKY}}(\mathbf{r}) d\mathbf{r}$. One finds, as expected, that J_{eff} decreases with increasing temperature due to the damping of the range function. Since the magnetic properties of the 2D system are directly dependent on J_{eff} , a finite T/T_F can have an important impact.

In the lattice MFT (where we have in mind the previously mentioned square lattice with lattice constant a), we calculate the Curie temperature with [5]

$$T_c = \frac{35}{12k_B} x \sum_{i=1}^{\infty} N_i J(r_i, T_c), \quad (3)$$

where N_i and r_i are the numbers and distances of the i th nearest neighbors, respectively. The continuum limit, which we examine first, is attained for $l, k_F^{-1} \gg a$, where a is the lattice spacing. We examine the large l limit ($l \gg k_F^{-1}$) and find that Eq. 3 becomes

$$\begin{aligned} T_c^* &= \frac{35\pi x \mathcal{J}_0}{6k_B} k_F^2 \int_0^{\infty} \chi(k_F r, T_c^*/T_F) r dr \\ &= \frac{35\pi x \mathcal{J}_0}{6k_B} g(T_c^*/T_F), \end{aligned} \quad (4)$$

where T_c^* is the Curie temperature in the continuum limit, and $g(T_c^*/T_F)$ depends only on the ratio of T_c^* to

the Fermi temperature T_F . For $T_c^* \ll T_F$, $g(T_c^*/T_F) \rightarrow 1$, and the dependence on carrier concentration is lost, and T_c^* depends only on the impurity concentration x . (For convenience, we identify this temperature as $T_c^\infty \equiv T_c(T_F \rightarrow \infty) = \frac{35\pi x \mathcal{J}_0}{6k_B}$.) This result, with no dependence on n_c , is proportional to the density of states at the Fermi Level E_F in two dimensions, and reflects the peculiarity of the 2D density of states being independent of carrier density. (The analogous continuum 3D result, also proportional to the density of states at E_F , is $T_c^* \propto x n_c^{1/3}$, and *does* depend on the carrier density). For the more general case of finite T_c^*/T_F , one can readily calculate the Curie temperature self-consistently via numerical means. Fig. 2 shows T_c^* curves as a function of carrier density for various values of x , the Mn concentration. A salient feature of the curves is a marked dependence on n_c , in contrast to what one finds when the ($T=0$) RKKY formula is used (where there is no dependence at all on n_c). Eventually, the curves saturate as n_c is increased. This is natural, since T_F increases with n_c , and ultimately T_c^*/T_F approaches zero. This $T_F \rightarrow \infty$ limit of the continuum MFT is the actual virtual approximation limit.

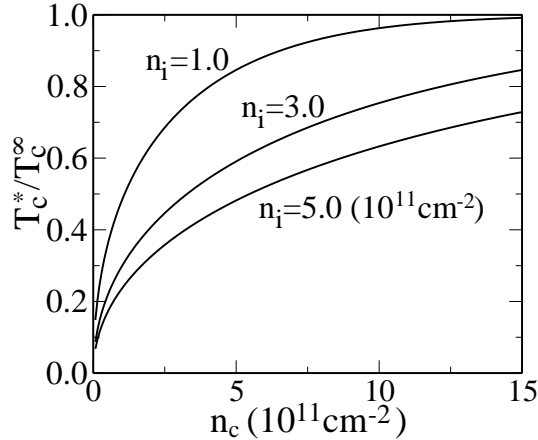


FIG. 2. 2D Curie temperature curves in the continuum MFT for various values of the magnetic impurity density n_i ($n_i = x a^{-2}$). Here T_c^∞ is the continuum T_c calculated for $T_F = \infty$, i.e. the virtual crystal approximation result.

Returning to the lattice MFT, which explicitly takes into account the discreteness of the square lattice, we also incorporate the effects of the finite carrier mean free path l by including an exponential cutoff in the range of the RKKY interaction. T_c curves are shown in Fig. 3 for several Mn dopant concentrations. As in Fig. 2, the Curie temperature increases monotonically in n_c over the experimentally accessible range of carrier densities. However, for considerably higher n_c (i.e. approaching 10^{14} cm^{-2}), nonmonotonic behavior is seen in T_c . This is evident in the inset of Fig. 3, where the Curie temperature curves seem to achieve saturation for intermediate carrier densities and ultimately begins to decrease as the

length scale k_F^{-1} of the RKKY oscillations shrinks relative to the lattice constant a . Eventually, for $k_F^{-1} \sim a$, the discrete nature of the lattice sum in Eq. 3 has a strong effect, leading to a considerably smaller T_c than the continuum value, T_c^* . This result for 2D T_c including disorder and finite temperature RKKY effects is one of our main new results.

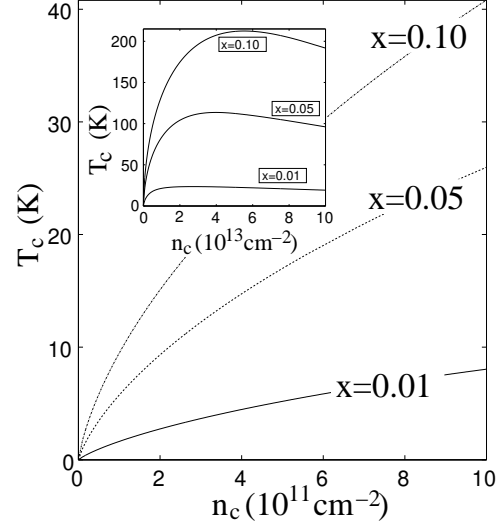


FIG. 3. Lattice MFT 2D Curie temperature curves for various values of x . In the inset, T_c curves are shown for a much greater range of carrier density n_c . In both the main graph and the inset, $l/a = 5$.

T_c is strongly affected by the finite size of l ; in fact, one sees that for each of the carrier concentrations represented in Fig. 4, T_c initially increases sharply with increasing l , eventually saturating for $l/a \gg 1$. It is informative to examine the regime $a \ll l, k_F^{-1}$, where one can operate in the continuum limit. We introduce $\eta \equiv k_F l$ as an important dimensionless variable; as will be seen, the ratio T_c^*/T_F tends to zero as η becomes small. For $T_c \ll T_F$ and $k_F r \ll 1$, a reasonable approximation for the finite temperature RKKY range function is $J^{RKKY}(r, T) \approx J^{RKKY}(r, 0)[(1 - a_2 \tau^2 - a_3 \tau^3) + (b_2 \tau^2 + b_3 \tau^3)(k_F r)]e^{-r/l}$ where $\tau \equiv T/T_F$, $a_2 = 0.2153$, $a_3 = -0.140$, $b_2 = -1.333$, and $b_3 = 0.862$ (The a_i and b_i have been calculated numerically). Since $J^{RKKY}(r, 0)$ varies slowly with $k_F r$ for small k_F , we can replace the Bessel functions in Eq. 2 with a series expansions in $k_F r$, and the result for small values of this expansion variable is

$$J^{RKKY}(r, T_c^*) \approx \mathcal{J}_0 k_F^2 / \pi [\alpha_1 + \alpha_2 (k_F r)^2] \times [1 - (a_2 \tau^2 + a_3 \tau^3) + (b_2 \tau^2 + b_3 \tau^3)(k_F r)] e^{-r/l}, \quad (5)$$

where $\alpha_1 \equiv [-1/2 + \gamma + \ln(k_F r/2)]$, and $\alpha_2 \equiv [-3/16 + \gamma/4 + 1/4 \ln(k_F r/2)]$; $\gamma = .57722 \dots$ is the Euler constant. In calculating T_c^* (in the continuum case), we assume that although $l \ll k_F^{-1}$, $l \gg a$. This additional condition allows the replacement of the discrete formula for the

Curie Temperature in Eq. 3 with the continuum version, and one has $T_c^* = x \frac{35\pi}{6} \int_0^\infty J^{RKKY}(r, T_c^*) r dr$. Carrying out the integration and solving for T_c^* , we find

$$T_c^* = \mathcal{J}_0 \frac{35x}{6k_B} \left\{ \eta^2 \left[\ln\left(\frac{2}{\eta}\right) - 1/2 \right] + \eta^4 \left[-\frac{41}{16} + \frac{1}{2} \ln\left(\frac{2}{\eta}\right) \right] \right\}, \quad (6)$$

where $\eta \equiv k_F l \ll 1$ and only terms up to fourth order in η are shown. The expression for T_c^* given in Eq. 6 reveals a strong suppression of T_c^* due to localization effects; when k_F is small (i.e. in the small n_c limit) the RKKY range function is very extended relative to a and l . As a consequence, most of the RKKY interaction is truncated by the exponential cutoff associated with the finite mean free path l . This truncation effect is so severe that T_c^* is very small in comparison with T_F ; to fourth order in η there are no corrections to arising from the finiteness of T_c^*/T_F . Note that in the opposite limit of $k_F l \gg 1$, which rarely applies to DMS systems which are at best “bad metals”, one can obtain the simple formula $T_c(k_F l \gg 1) \approx T_c^*[1 - (k_F l)^{-1}/\pi]$ by simply considering the disorder induced suppression of the 2D density of states.

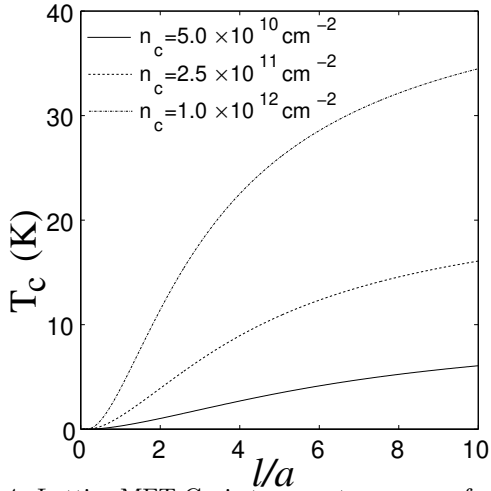


FIG. 4. Lattice MFT Curie temperature curves for various values of n_c plotted as a function of the mean free path l/a . In each case the same Mn concentration, $x = .05$, is used.

In addition to T_c , one can also use lattice MFT to calculate the magnetization $M(T)$ [5]. The magnetization behavior is influenced by the Mn impurity concentration as well as the form of the effective interaction between Mn local moments, in principle specified by the carrier mean free path l and n_c . For convenience, we study $M(T/T_c)$; using the normalized temperature scale T/T_c allows a systematic comparison of magnetization profiles corresponding to different values of the parameters l , n_c , and x . An important trait of the magnetization profile is its degree of *concavity*; concavity in $M(T)$ is a hallmark of an insulating system, while a convex profiles occur

well within the metallic regime [4]. Linear magnetization curves correspond to intermediate impurity densities and mean free paths. In terms of the magnetization, the concavity γ is given by $\gamma \equiv \int_{t_1}^{t_2} M''(T) dT$, or the difference in the slopes of $M(T)$. The sign of γ indicates whether $M(T)$ is convex (negative γ), concave (positive γ), or linear (if $\gamma \approx 0$). The temperatures t_1 and t_2 are selected to encompass an intermediate temperature range, neither too close to T_c nor to zero. A significant feature of the concavity plots shown in Fig. 5 is weak dependence of the concavity of the magnetization profiles on the carrier density; though the three values of n_c range over two orders of magnitude ($10^{10} - 10^{12}$) cm^{-2} , the γ graphs lie very close to one another. One can also see that the parameter range over which the $M(T)$ profile is concave is much more extensive than predicted by lattice MFT for three dimensional DMS systems [5]. This is primarily a consequence of the geometry of the two dimensional lattice. The insets of the graphs in Fig. 5 display representative cases of the magnetization $M(T)$.

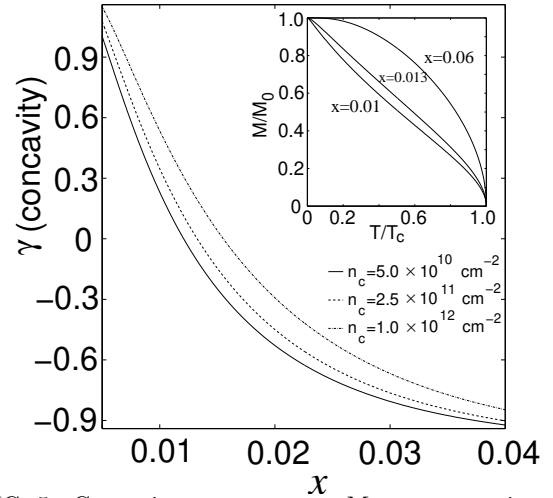


FIG. 5. Concavity curves versus Mn concentration x for several carrier densities n_c with $l/a = 2.0$. The inset shows representative examples of the magnetization, $M(T)$. All $M(T)$ curves are calculated for $n_c = 2.5 \times 10^{11} \text{ cm}^{-2}$.

In conclusion, we have considered diluted magnetic semiconductors in two dimensions. We have found that, even at the level of continuum MFT, finite temperature effects in the carrier-mediated effective interaction between Mn impurity moments introduce a strong dependence on the density of carriers, where naive use of the zero temperature RKKY formula yields a result independent of n_c . To take into account the discreteness of the strong positional disorder of the 2D DMS system, we have employed a lattice MFT. Our lattice theory also provides a convenient framework for the inclusion of important physics such as the finite mean free path. In general, the 2D DMS T_c is strongly suppressed compared with the corresponding 3D DMS T_c , which is somewhat

discouraging for spintronic applications.

This work is supported by US-ONR and DARPA.

- [1] T. Dietl *et al.*, Phys. Rev. B **63**, 195205 (2001); C. Timm, J. Phys.: Condens. Matter **15** 1865 (2003).
- [2] H. Ohno *et al.*, Nature **402**, 790 (1999).
- [3] A. Nazmul *et al.*, Phys. Rev. B **67**, 241308 (2003).
- [4] S. Das Sarma *et al.*, Phys. Rev. B **67**, 155201 (2003); Solid State Comm. **127**, 99 (2003).
- [5] D.J. Priour *et al.*, Phys. Rev. Lett. **92**, 117201(2004).
- [6] B. Lee *et al.*, Phys. Rev. B **61**, 15606(2000).
- [7] D. N. Aristov, Phys. Rev. B **55**, 8064 (1997).